Kinetics of Complex Isothermal Reversible First-Order Reaction Systems Involving Three Components

LARRY E. FAITH and THEODORE VERMEULEN

University of California, Berkeley, California

A new calculation method presented here for interpreting batch or tubular-flow reactor data (and also CSTR data) on three-component, three-reaction reversible systems is based upon the general analyses of Jost and of Wei and Prater. With advance knowledge of the pertinent equilibria, even a very few experimental points can be matched easily and rapidly to the given figures and equations. The simplification involved when one reaction disappears, with the divariant system thus becoming monovariant, is also described. Representative concentration-time curves are given for design purposes.

Several ways exist for analyzing complex reaction systems, some general and some rather specific. For a pair of consecutive irreversible reactions involving three components, Jungers et al. (5) have presented graphs that can be used for numerical solutions for batch reactors or for tubular-flow conditions. Levenspiel (6) describes applicable procedures for such reactions and includes a treatment for the continuous stirred-tank reactor. Chien (2) and Chermin and van Krevelen (1) have analyzed reaction systems involving three components having various orders for the two reaction steps.

Siewert et al. (9) have developed graphs for analyzing consecutive reactions involving three components, having one reversible step and one irreversible step. Both tubular-flow and continuous stirred-tank reactors are covered, with two of the three rates being first order and the third either first or second order. Lowry and John (7) have given algebraic solutions for two consecutive irreversible reactions in tubular flow or batch, where all steps are first order. Vriens (10) provides equations for coupled reversible reactions, either consecutive or competitive.

Rodiguin and Rodiguina (8) have extended this type of analysis to a large number of consecutive and competitive reversible steps. From a still more general approach, Jost (4) and Wei and Prater (12) have presented a matrix method for analyzing first-order reaction systems involving any number of mutually accessible components. Wei (11) extended this method to include reactors with a distribution of residence times, including the continuous stirred-tank reactor.

The following new method for analyzing three-component reaction systems, based on the analysis by Wei and Prater, is applicable to all reversible first-order, three-component systems. It is more specific and direct than the preceding analyses, because in it the degree of variability is recognized, and this is used to identify the minimum required number of experimental points. The most difficult problem in kinetics is to interpret experimental data. In this new method, the needed kinetic parameters can almost always be solved from as few as three composition points along a single reaction path, *with the corresponding reaction times,* in addition to the equilibrium and starting compositions.

REACTION STEPS KNOWN AND RATES KNOWN

Figure 1, adapted from Wei and Prater, is the composition diagram for the following three-component reaction system:

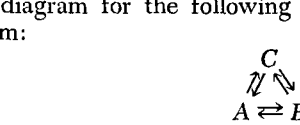

The reaction steps are first order, with the stoichiometry the same as the kinetics. Reaction is assumed to occur at constant density and constant temperature. For a given set of six rate coefficients, the contours show the reaction path toward equilibrium, starting from any nonequilibrium composition on the entire diagram. This type of contour map, for a given chemical system, can only be calculated when the equilibrium and kinetic parameters have all been determined.

Larry E. Faith is with Shell Development Company, Emeryville, California.

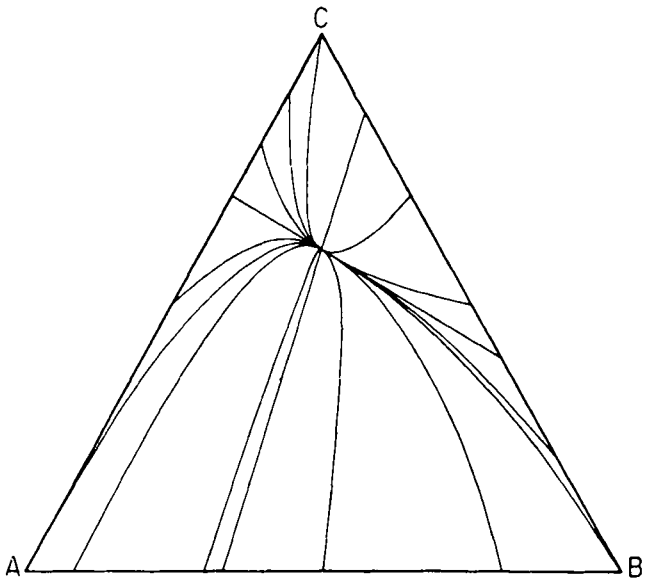

Fig. 1. Typical reaction paths for a three-component reaction system.

In the Wei and Prater method, a sequence of experimental runs is made, in which the starting composition for a preplanned run is determined by drawing the apparent tangent (at the equilibrium point) to the experimental reaction-path curve from the preceding run, and extending the tangent to the edge of the diagram. Eventually a reaction path that is a straight line is found. After this straight line, or characteristic line, is located, the other characteristic line can be calculated and the rate coefficients determined.

The general three-component reaction system has six rate coefficients associated with it, as shown in Figure 1. In conformity with microscopic reversibility, the three forward rate coefficients (k's) are related to the respective reverse coefficients (k''s) by the equilibrium constants (K's):

$$K_{AB} = \frac{1}{K'_{AB}} = \frac{k_{AB}}{k'_{AB}} \tag{1}$$

$$K_{BC} = \frac{1}{K'_{BC}} = \frac{k_{BC}}{k'_{BC}} \tag{2}$$

$$K_{CA} = \frac{1}{K'_{CA}} = \frac{k_{CA}}{k'_{CA}} \tag{3}$$

(Subscript letters on the forward steps indicate reactant first, then product, reversing the sequence used by Wei and Prater.) For Figure 1 specifically, Wei and Prater have given the parameters

$$K_{AB} = 1 \qquad k_{AB} = 1$$
$$K_{BC} = 3 \qquad k_{BC}/k_{AB} = 33$$
$$K_{CA} = 1/3 \qquad k_{CA}/k_{AB} = 18.5$$

The three equilibrium constants are related, so that only two are independent:

$$K_{AB}K_{BC}K_{CA} = 1 \tag{4}$$

For known equilibrium, the six rate coefficients reduce to three independent unknown parameters. Here these parameters are selected to be a single forward rate coefficient and two ratios involving the three forward rate coefficients, for example, k_{AB}, k_{BC}/k_{AB}, and k_{CA}/k_{AB}. The reaction path on a triangular composition diagram depends only on the two ratios, each of which must be positive. Hence the reaction system is called a *divariant* system.

Many reaction systems involving three components are not as general as the divariant system. Often one of the reaction steps does not occur; then the system simplifies to one of the following monovariant, or noncyclic, types:

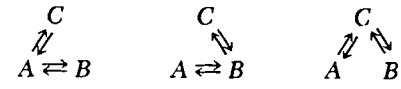

Although the assignment of component numbers is arbitrary, it is necessary to consider this group of reactions as separate possibilities, so as to compare their combined behavior with that of a divariant system. For this reason they are designated in sequence as type I, type II, and type III. The number of independent rate coefficients reduces to two in these noncyclic cases. The reaction path on a triangular composition diagram depends only on the ratio of rate coefficients for the two steps, and the noncyclic reaction system is termed *monovariant*.

REACTION STEPS KNOWN AND RATES UNKNOWN

For an experimental multireaction system, usually the starting and equilibrium compositions are readily known, but not the constants that define the reaction path between them. At this stage of the problem, many paths between these two compositions are possible. All such paths lie within a restricted region of the three-component diagram, which is established only by the starting and equilibrium compositions.

The determination of the unknown rate ratios that govern a reaction path is equivalent to comparing the observed reaction path with each of the possible paths between the starting composition and the equilibrium to determine which one it matches best. Thus Figures 2 to 5 which follow are curves showing a range of possible reaction paths—possible in the sense that no comparison has yet been made with experiment—for a specified starting composition and known equilibrium. (Each of these systems has the same equilibrium composition as the system in Figure 1.) By contrast Figure 1 is a contour family of reaction paths for all possible starting points, for one specified set of rate ratios.

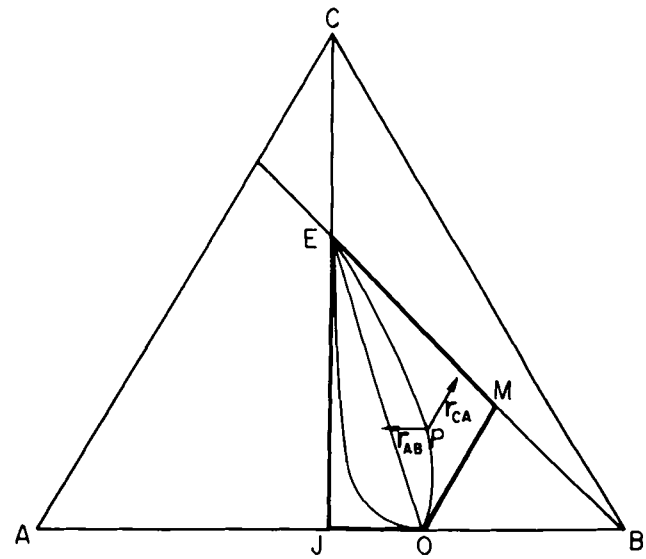

Fig. 2. Region of allowable reaction paths for a type I monovariant reaction system, starting from a specified composition O.

Consider the *monovariant* system in Figure 2, which corresponds to type I. Point O is the starting composition of an experimental run and point E is the equilibrium. At any composition on the diagram the reaction rate is the vector sum of two partial vectors, each one representing the net rate for one of the two reaction steps. At point P the partial vector r_{AB} represents the net rate from species A to species B. It lies parallel to the isoconcentration line (isocon) OJ, is directed toward the equilibrium line JE, and has a magnitude proportional to the net rate of the AB reaction step. The partial vector r_{CA} represents the net rate from species C to species A. It is parallel to the isocon OM, and is directed toward the equilibrium line ME.

If the reaction between components A and B is very fast, the composition travels along isocon OJ, and then moves slowly along the equilibrium line JE. In this case k_{CA}/k_{AB} is zero. If the reaction between components A and C predominates, then rapid equilibrium is attained along isocon OM, followed by a slower reaction along the equilibrium line ME. In this case k_{CA}/k_{AB} is infinite. Intervening reaction paths all have finite values of k_{CA}/k_{AB}, and are all contained in the quadrilateral $OJEM$. (The reaction paths shown have not been calculated, but are schematic.)

The irreversible consecutive reaction system considered by Levenspiel (*4*) and many others is a monovariant system entirely analogous to this type. For this variant of the present case, point O would move to vertex B, point J to vertex A, and point E to vertex C; thus the applicable reaction sequence would be $B \rightarrow A \rightarrow C$.

The type II monovariant system shown in Figure 3 has a rate vector which can be resolved into vectors r_{AB} and r_{BC}, as shown at point P. These vectors represent the net rates between components A and B and between components B and C, respectively.

If a reaction proceeds from starting composition O to equilibrium composition E, the path will follow some curve lying within the envelope $OJLEN$. If k_{BC}/k_{AB} is very large, the composition proceeds along isocon OL and then slowly along equilibrium line LE. If k_{BC}/k_{AB} is zero, isocon OJ and equilibrium line JE constitute the asymptotic reaction path. The other possible reaction paths begin at point O, move to the left, and curve upward, away from isocons OJ and ON. To the right of equilibrium line JE, neither r_{AB} nor r_{BC} changes direction. Thus all paths cross this line, at which time r_{AB} is zero. After this time, r_{AB} is directed toward the right, which prevents the reaction paths from crossing equilibrium line LE before reaching point E.

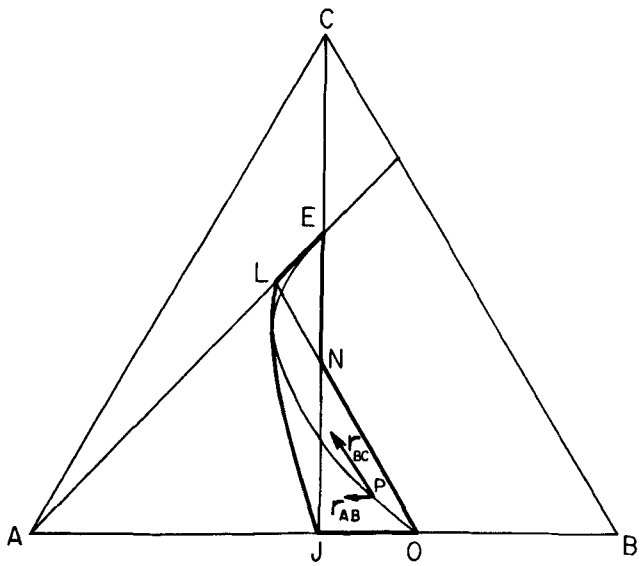

Fig. 3. Region of allowable reaction paths for a type II monovariant reaction system, starting from a specified composition O.

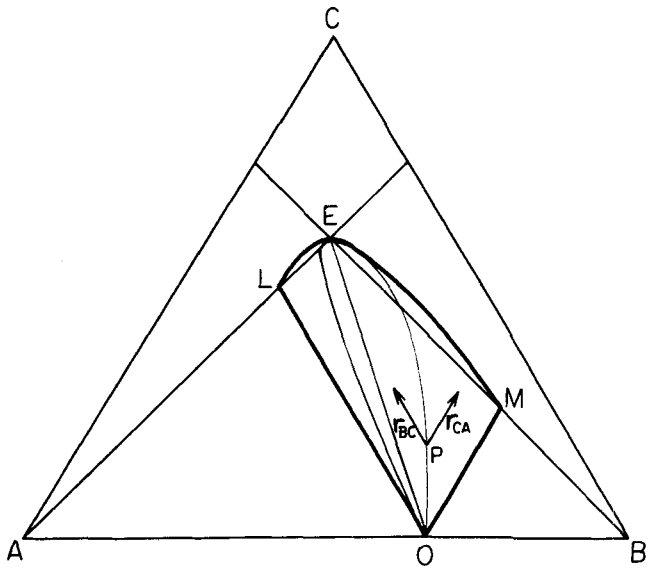

Fig. 4. Region of allowable reaction paths for a type III monovariant reaction system, starting from a specified composition O.

The type III monovariant system shown in Figure 4 has a rate vector that combines r_{BC} and r_{CA}. If k_{CA}/k_{BC} is very large, the asymptotic reaction path is OME. OLE is the asymptotic path if k_{CA}/k_{BC} is zero. Other reaction paths begin at composition O and move upward. During this time components A and B are being transformed into component C. There is nothing to prevent one of these steps from reaching its partial equilibrium momentarily, and then having its net direction reversed due to the progress of the other reaction step. Later it will be proved that for all curved reaction paths, in this case, one of the two reaction steps must change its direction during the course of a reaction. Thus each curved reaction path crosses an equilibrium line, LE or ME, before reaching equilibrium. All reaction paths are contained within an envelope curve LEM and the two isocons OL and OM. The envelope is smooth, and a tangent at point E can be related to the straight-line reaction path OE by a method to be given later.

As equilibrium is approached in each of the three monovariant systems, the reaction proceeds in such a way that the component at one end of the chain is decreasing in concentration, while the concentration of the component at the other end is increasing. For example, in Figure 4, along the paths left of the straight line OE, *near equilibrium*, there is a net reaction from species A through species C to species B; along the paths to the right of line OE, the net reaction occurs from species B toward species A.

The reaction paths in the three monovariant systems form a continuous family of curves, which extend from the reaction path OME through the curves in Figure 2 to reaction path OJE, and from this path through the curves in Figure 3 to the asymptotic path OLE, and from this path through the curves in Figure 4 back to the asymptotic path OME. As the reaction paths in the three systems approach equilibrium, they form a single family of lines radiating from point E over an angle of 180 deg.

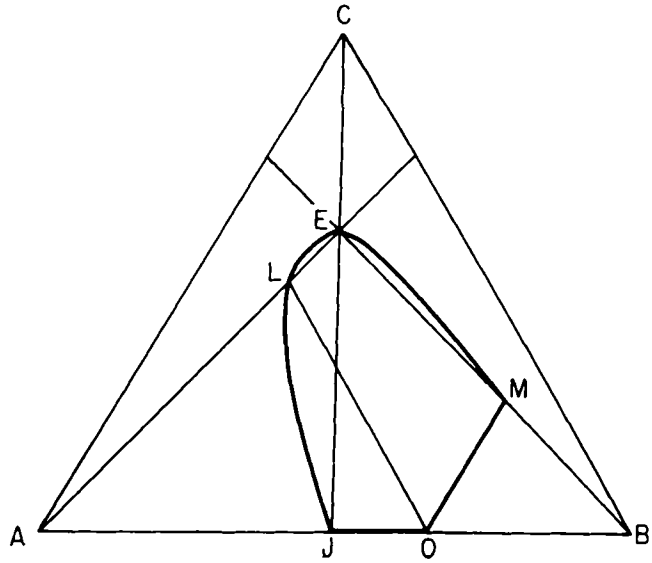

Fig. 5. Region of allowable reaction paths for a divariant reaction system, starting from a specified composition O.

The boundaries for all possible reaction paths in the monovariant systems provide the limiting curves for the double infinitude of permissible paths in the divariant system. This region is enclosed by the heavy boundary *OJLEM* in Figure 5.

RATE EQUATIONS

Equations (5) are the batch rate equations for the three-component divariant reaction system typified by Figure 1:

$$\left.\begin{aligned}\frac{dx_A}{dt} &= -(k_{AB}+k_{CA}^{\dagger})x_A + k_{AB}^{\dagger}x_B + k_{CA}x_C \\ \frac{dx_B}{dt} &= +k_{AB}x_A - (k_{AB}^{\dagger}+k_{BC})x_B + k_{BC}^{\dagger}x_C \\ \frac{dx_C}{dt} &= k_{CA}^{\dagger}x_A + k_{BC}x_B - (k_{CA}+k_{BC}^{\dagger})x_C\end{aligned}\right\} \quad (5)$$

where x_A, etc., designate the mole fraction of each component, relative to the total concentration of all three components; that is, $x_A + x_B + x_C = 1$. Wei and Prater have derived the general solution for the foregoing system:

$$x_A - x_{Ae} = \frac{1}{u_2-u_1}\{[(x_{AO}-x_{Ae}) + u_1(x_{BO}-x_{Be})]u_2e^{-\lambda_1 t} - [(x_{AO}-x_{Ae}) + u_2(x_{BO}-x_{Be})]u_1e^{-\lambda_2 t}\} \quad (6a)$$

$$x_B - x_{Be} = \frac{1}{u_2-u_1}\{-[(x_{AO}-x_{Ae}) + u_1(x_{BO}-x_{Be})]e^{-\lambda_1 t} + [(x_{AO}-x_{Ae}) + u_2(x_{BO}-x_{Be})]e^{-\lambda_2 t}\} \quad (6b)$$

$$x_C - x_{Ce} = -(x_A - x_{Ae}) - (x_B - x_{Be}) \quad (6c)$$

where

$$\lambda_1 = \frac{\kappa_a+\kappa_b+\sqrt{\Delta}}{2}; \quad \lambda_2 = \frac{\kappa_a+\kappa_b-\sqrt{\Delta}}{2}$$

$$u_1 = \frac{\kappa_a-\kappa_b-\sqrt{\Delta}}{2\kappa_c}; \quad u_2 = \frac{\kappa_a-\kappa_b+\sqrt{\Delta}}{2\kappa_c}$$

and

$$\Delta = (\kappa_a-\kappa_b)^2 + 4\kappa_c\kappa_d$$

For given equilibrium behavior, with three independent rate coefficients

$$\kappa_a = k_{CA} + k_{CA}^{\dagger} + k_{AB} = k_{CA}(1+K_{CA}^{\dagger}) + k_{AB}$$

$$\kappa_b = k_{BC} + k_{BC}^{\dagger} + k_{AB}^{\dagger} = k_{BC}(1+K_{BC}^{\dagger}) + k_{AB}K_{AB}^{\dagger}$$

$$\kappa_c = k_{AB} - k_{BC}^{\dagger} = k_{AB} - k_{BC}K_{BC}^{\dagger}$$

$$\kappa_d = k_{AB}^{\dagger} - k_{CA} = k_{AB}K_{AB}^{\dagger} - k_{CA}$$

The equilibrium concentrations x_{Ae} and x_{Be} account for two degrees of freedom in the rate coefficients. The three remaining degrees of freedom are specified by the paramters λ_1, λ_2, and u_1 or u_2.

The interdependence of u_1 and u_2 can be established in the following way. From the above definitions

$$u_1 + u_2 = \frac{\kappa_a-\kappa_b}{\kappa_c}; \quad u_2 - u_1 = \frac{\sqrt{\Delta}}{\kappa_c} \quad (7a)$$

$$u_1u_2 = -\frac{\kappa_d}{\kappa_c} \quad (7b)$$

Hence

$$u_1 + u_2 = \frac{k_{AB}}{\kappa_c}\left\{(-K_{AB}^{\dagger}+1) - \frac{k_{BC}}{k_{AB}}(K_{BC}^{\dagger}+1) + \frac{k_{CA}}{k_{AB}}(K_{CA}^{\dagger}+1)\right\} \quad (8)$$

The rate ratios k_{BC}/k_{AB} and k_{CA}/k_{AB} can be evaluated in terms of κ_d and κ_c, respectively. Substitution in Equation (8) gives

$$u_1 + u_2 = 1 + \frac{1}{K_{BC}^{\dagger}} - \frac{\kappa_d}{\kappa_c}(1+K_{CA}^{\dagger}) = 1 + K_{BC} + u_1u_2(1+K_{CA}^{\dagger}) \quad (9)$$

Solution for u_2 in terms of u_1 then gives

$$u_2 = \frac{1+K_{BC}-u_1}{1-u_1(1+K_{CA}^{\dagger})} \quad (10)$$

It is noted that u_1 and u_2 are interchangeable in this equation.

Differentiation of Equations (6*a*) and (6*b*) gives the following rate relations:

$$\frac{dx_A}{dt} = \frac{1}{u_2-u_1}\{-[(x_{AO}-x_{Ae}) + u_1(x_{BO}-x_{Be})]u_2\lambda_1e^{-\lambda_1 t} + [(x_{AO}-x_{Ae}) + u_2(x_{BO}-x_{Be})]u_1\lambda_2e^{-\lambda_2 t}\} \quad (11a)$$

$$\frac{dx_B}{dt} = \frac{1}{u_2-u_1}\{[(x_{AO}-x_{Ae}) + u_1(x_{BO}-x_{Be})]\lambda_1e^{-\lambda_1 t} - [(x_{AO}-x_{Ae}) + u_2(x_{BO}-x_{Be})]\lambda_2e^{-\lambda_2 t}\} \quad (11b)$$

The significance of the two exponential terms in these two equations will now be explained. For this purpose, use is made of Figure 6, which shows a three-component reaction system with two characteristic lines QQ and SS passing through the equilibrium point E. Line QQ is described by

$$x_A - x_{Ae} = -u_2(x_B - x_{Be}) \quad (12)$$

Line SS corresponds to

$$x_A - x_{Ae} = -u_1(x_B - x_{Be}) \quad (13)$$

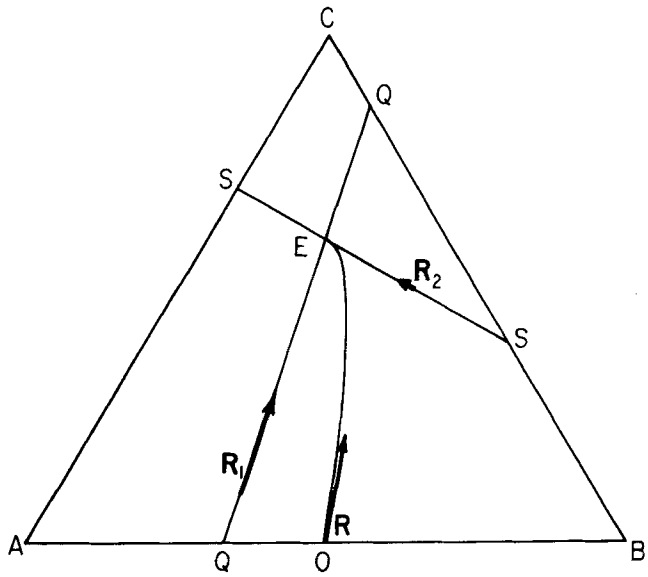

Fig. 6. Rate vectors for a typical three-component reaction system.

Straight-Line Reaction Paths

Suppose that a composition at the start of a reaction satisfies Equation (12), in the form

$$(x_{AO} - x_{Ae}) + u_2(x_{BO} - x_{Be}) = 0 \qquad (14)$$

Then Equations (6*a*) and (6*b*) simplify because the coefficients of $e^{-\lambda_2 t}$ vanish, and the reaction path becomes

$$x_A - x_{Ae} = (x_{AO} - x_{Ae})\, e^{-\lambda_1 t} \qquad (15)$$

$$x_B - x_{Be} = (x_{BO} - x_{Be})\, e^{-\lambda_1 t} \qquad (16)$$

Thus the composition will then follow the characteristic line QQ toward equilibrium throughout the reaction. The corresponding rate equations are

$$\frac{dx_A}{dt} = -(x_{AO} - x_{Ae})\,\lambda_1 e^{-\lambda_1 t} = -\lambda_1(x_A - x_{Ae}) \qquad (17)$$

$$\frac{dx_B}{dt} = -(x_{BO} - x_{Be})\,\lambda_1 e^{-\lambda_1 t} = -\lambda_1(x_B - x_{Be}) \qquad (18)$$

In Figure 6 $\mathbf{R}_1$ is a vector representing the reaction rate for this path. It has two component vectors whose magnitudes are given by Equations (17) and (18).

Alternately, if Equation (13) is satisfied by the initial composition, then Equations (6*a*) and (6*b*) reduce to

$$x_A - x_{Ae} = (x_{AO} - x_{Ae})\, e^{-\lambda_2 t} \qquad (19)$$

$$x_B - x_{Be} = (x_{BO} - x_{Be})\, e^{-\lambda_2 t} \qquad (20)$$

$\mathbf{R}_2$ in Figure 6 is a rate vector directed along line SS, that has two component vectors with magnitudes

$$\frac{dx_A}{dt} = -(x_{AO} - x_{Ae})\,\lambda_2 e^{-\lambda_2 t} = -\lambda_2(x_A - x_{Ae}) \qquad (21)$$

$$\frac{dx_B}{dt} = -(x_{BO} - x_{Be})\,\lambda_2 e^{-\lambda_2 t} = -\lambda_2(x_B - x_{Be}) \qquad (22)$$

Curved Reaction Paths

If the initial composition of a reaction system does not lie on either characteristic line, as is the case for point O in Figure 6, then Equations (6*a*), (6*b*), (11*a*), and (11*b*) will describe the composition and rate of the system as a function of time. In Figure 6 the rate is represented by the vector $\mathbf{R}$, which has two constituent vectors with magnitudes given in Equations (11*a*) and (11*b*). On the right side of these equations, the first exponential terms are magnitudes of the components of $\mathbf{R}_1$ displaced to point O. The second exponential terms are the magnitudes of the $\mathbf{R}_2$ components displaced to point O. Thus $\mathbf{R}$ is a vector sum of $\mathbf{R}_1$ and $\mathbf{R}_2$. In other words, the reaction rate along the path OE can be described as the resultant of two independent rates, each having the direction of one of the characteristic lines, for which λ_1 and λ_2 are the respective rate coefficients. As $\lambda_1 > \lambda_2$, $\mathbf{R}_1$ approaches zero faster than $\mathbf{R}_2$, and all curved reaction paths become tangent to the line SS as equilibrium is approached.

INTEGRATED RATE EQUATIONS IN DIMENSIONLESS FORM

Let F_A and F_B be dimensionless measures of the concentrations of species A and B, as fractional departures of concentration from equilibrium:

$$F_A = \frac{x_A - x_{Ae}}{x_{AO} - x_{Ae}} \qquad (23)$$

$$F_B = \frac{x_B - x_{Be}}{x_{BO} - x_{Be}} \qquad (24)$$

Also the parameter H is taken as the ratio of the two initial departures from equilibrium:

$$H = \frac{x_{BO} - x_{Be}}{x_{AO} - x_{Ae}} \qquad (25)$$

Combination of Equations (23) to (25) and (6*a*) and (6*b*) gives

$$F_A = \frac{1}{(u_2 - u_1)}\left[(1 + u_1 H)u_2 e^{-\lambda_1 t} - (1 + u_2 H)u_1 e^{-\lambda_2 t}\right] \qquad (26)$$

$$F_B = \frac{1}{(u_2 - u_1)H}\left[-(1 + u_1 H)e^{-\lambda_1 t} + (1 + u_2 H)e^{-\lambda_2 t}\right] \qquad (27)$$

Parameters U and V are then defined as

$$U = \frac{u_1(1 + u_2 H)}{u_2 - u_1} \qquad (28)$$

$$V = -\frac{U}{u_1 H} = -\frac{1 + u_2 H}{H(u_2 - u_1)} \qquad (29)$$

The terms in u_1, u_2 and H in Equations (26) and (27) can be entirely replaced by terms in U and V:

$$F_A = (1 + U)\, e^{-\lambda_1 t} - U\, e^{-\lambda_2 t} \qquad (30)$$

$$F_B = (1 + V)\, e^{-\lambda_1 t} - V\, e^{-\lambda_2 t} \qquad (31)$$

Master Plots

It is desirable to find a conversion variable that can be plotted as a function of a time variable and a contour parameter. It will now be shown that U (or V) can be used as this type of contour parameter. Division of Equation (31) by Equation (30) gives

$$\frac{F_B}{F_A} = \frac{1 + V(1 - e^{(\lambda_1 - \lambda_2)t})}{1 + U(1 - e^{(\lambda_1 - \lambda_2)t})} \qquad (32)$$

Subtraction from unity then gives

$$1 - \frac{F_B}{F_A} = \frac{(U - V)\,[1 - e^{(\lambda_1 - \lambda_2)t}]}{1 + U\,[1 - e^{(\lambda_1 - \lambda_2)t}]} = \frac{(1 - V/U)\;U[1 - e^{(\lambda_1 - \lambda_2)t}]}{1 + U\,[1 - e^{(\lambda_1 - \lambda_2)t}]} \qquad (33)$$

A concentration variable Q is now defined as

$$Q = \frac{1 - F_B/F_A}{1 - V/U} = \left(\frac{u_1 H}{1 + u_1 H}\right)\left(1 - \frac{F_B}{F_A}\right) \quad (34)$$

with $V = -U/u_1 H$ as in Equation (29). Also a time variable T/U is selected, such that

$$T/U = (\lambda_2 - \lambda_1)t \quad (35)$$

and

$$Q = \frac{U(1 - e^{-T/U})}{1 + U(1 - e^{-T/U})} \quad (36)$$

Since U depends upon u_1, u_2, and H, and u_2 is related to u_1 by Equation (10), U is a function only of u_1 and H.

For extracting the lumped rate coefficient λ_1 or λ_2 it is necessary to compute the time behavior of the constituent vector $\mathbf{R}_1$ or $\mathbf{R}_2$. For example, $\mathbf{R}_1$ (dependent upon λ_1) can be extracted from Equations (26) and (27) in the following way. These relations, with the former multiplied by $(u_2 - u_1)$ and the latter by $u_1 H(u_2 - u_1)$, can be written as

$$(u_2 - u_1)F_A = (1 + u_1 H)u_2 e^{-\lambda_1 t} - (1 + u_2 H)u_1 e^{-\lambda_2 t} \quad (37)$$

$$u_1 H(u_2 - u_1)F_B = -(1 + u_1 H)u_1 e^{-\lambda_1 t} + (1 + u_2 H)u_1 e^{-\lambda_2 t} \quad (38)$$

Addition, with division by $(u_2 - u_1)(1 + u_1 H)$, gives the ratio F_1:

$$F_1 = \frac{F_A + u_1 H F_B}{1 + u_1 H} = e^{-\lambda_1 t} \quad (39a)$$

The corresponding ratio F_2 is obtained similarly:

$$F_2 = \frac{F_A + u_2 H F_B}{1 + u_2 H} = e^{-\lambda_2 t} \quad (39b)$$

Dimensionless Plots

Figures 7 and 8 have been calculated from Equation (36), and show Q (or $|Q|$) as ordinate with a family of U values. From the definitions of λ_1 and λ_2 following Equations (6), always $\lambda_1 > \lambda_2$, and hence T/U $(= -(\lambda_1 - \lambda_2)t)$ is always negative. Figure 7, with T as abscissa, holds for negative values of U and positive values of T. Figure 8 applies for the opposite case, with positive U and negative T. In the latter case Q reverses sign as $|T|$ increases, going to $-\infty$ and returning from $+\infty$. For plotting convenience this cusp has been used as an axis in Figure 8, where the abscissa is the parameter T':

$$T' = T/(T)_{Q=\infty} \quad (40)$$

Equation (36) shows that at small $|T|$, $Q \approx UT/U = T$. At large $|T|$, Q approaches an asymptotic value of 1. At the cusp of Figure 8, where the denominator of Equation (36) is zero

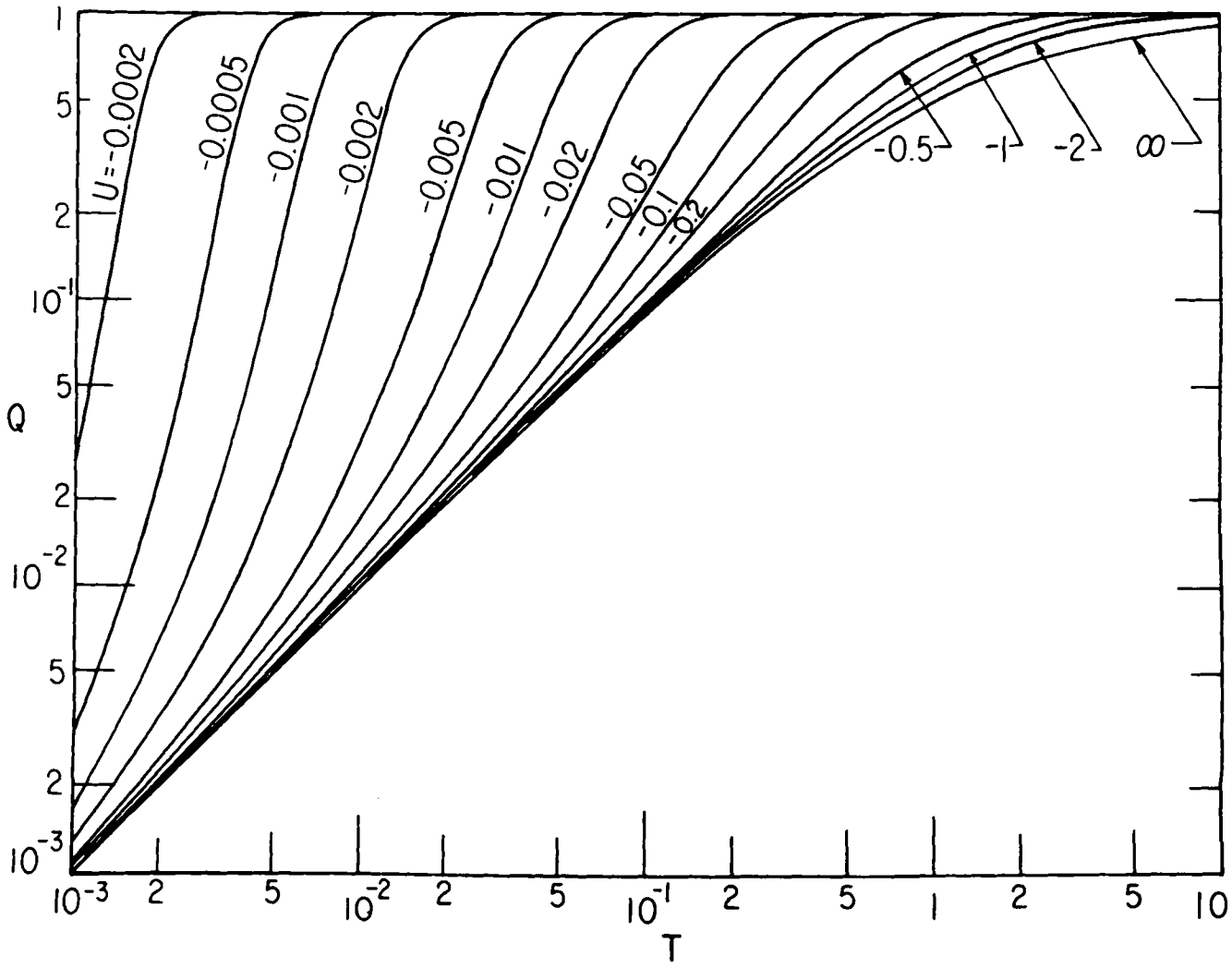

Fig. 7. Dimensionless master plot with negative U values as contours.

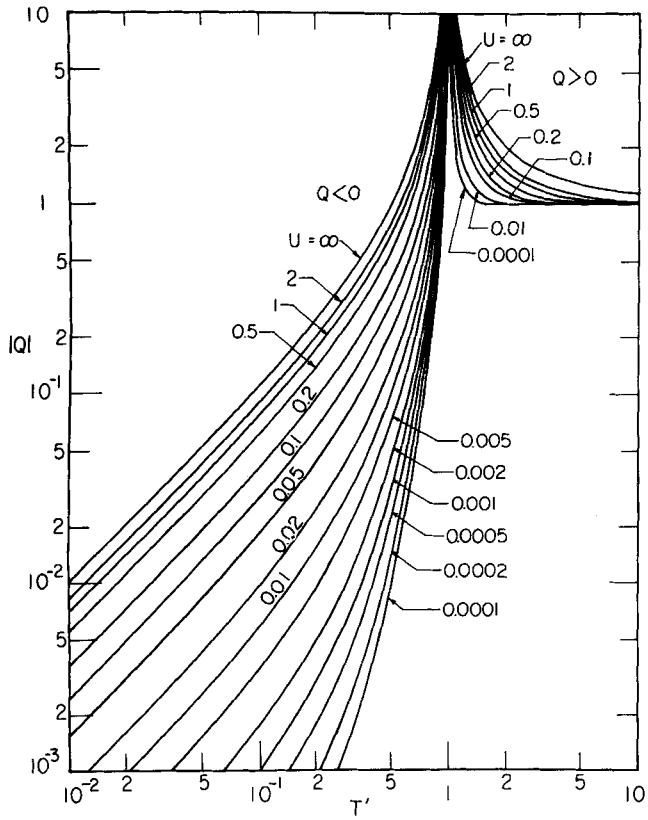

Fig. 8. Dimensionless master plot with positive U values as contours.

$$(T)_{Q=\infty} = +U \ln [U/(1+U)] \qquad (41)$$

For the limit of U = ∞, Equation (36) reduces to

$$Q = T/(1+T) \qquad (42)$$

Approach to Equilibrium

The evaluation of u_1 at compositions in the region close to equilibrium will now be investigated for all possible reaction systems which fit the initial and equilibrium compositions, points O and E, in Figure 9. H is positive valued for these compositions. For the limit of $t = \infty$, Equation (36) reduces to

$$(Q)_{t=\infty} = 1 \qquad (43)$$

Equation (34) then simplifies to

$$u_1 = -\frac{1}{H}\left(\frac{F_A}{F_B}\right)_{t=\infty} = -\left(\frac{x_A - x_{Ae}}{x_B - x_{Be}}\right)_{t=\infty} \qquad (44)$$

which is the equation for characteristic line SS of Figure 6, given earlier as Equation (13). All possible reaction paths converge at point E in the 180-deg. sector that lies below line WW', the tangent to enveloping curve $JLEM$ shown in Figure 5. In rotating clockwise through this semicircle, u_1 continually decreases, except over isocon $I'I'$, where u_1 has a discontinuity in changing from $-\infty$ to $+\infty$. Along isocon II, u_1 is zero. As line WW' is approached, that is, as the u_1 characteristic line approaches line WW', the u_2 characteristic line is approaching line OE. Hence the slope of line WW' can be obtained as a particular $-u_1$, by Equation (10), by taking the corresponding $-u_2$ as the slope of line OE $(= 1/H)$:

$$-\left(\frac{x_A - x_{Ae}}{x_B - x_{Be}}\right)_{WW'} = \frac{1 + H(K_{BC}+1)}{H + K^{\dagger}_{CA} + 1} \qquad (44a)$$

Figure 9 shows the intervals of u_1 values in the various regions close to equilibrium.

For the three monovariant systems, the ranges of applicable u_1 values are bounded by values of u_1 for the three pseudo-equilibrium lines:

$$u_1 = -K^{\dagger}_{AB} \quad \text{along } CC'$$

$$u_1 = K_{BC} + 1 \quad \text{along } AA'$$

$$u_1 = 1/(K^{\dagger}_{CA} + 1) \quad \text{along } BB'$$

From the regions of permissible reaction paths for these initial and equilibrium compositions, $-1/K_{AB} < u_1 < 1/(K^{\dagger}_{CA} + 1)$ for the type I monovariant system, and either $u_1 > (K_{BC} + 1)$ or $u_1 < -1/K_{AB}$ for the type II system.

For the type III system, $1/(K^{\dagger}_{CA} + 1) < u_1 < (K_{BC} + 1)$; that is, the reaction paths for this system converge to equilibrium in the sectors bounded by angles AEW and MEW'. This can be shown by starting from the basic definitions. For this system, $\kappa_a = k_{CA}(K^{\dagger}_{CA} + 1)$, $\kappa_b = k_{BC}(K^{\dagger}_{BC} + 1)$, $\kappa_c = -k_{BC}K^{\dagger}_{BC}$, and $\kappa_d = -k_{CA}$. Since both κ_c and κ_d are negative, $u_1 > 0$. The definition of u_1 corresponds to

$$u_1 = \frac{\kappa_a - \kappa_b - [(\kappa_a - \kappa_b)^2 + 4\kappa_c\kappa_d]^{1/2}}{2\kappa_c} \qquad (45)$$

Transposing $(\kappa_a - \kappa_b)/2\kappa_c$ and squaring both sides, we obtain

$$\left[u_1 - \frac{\kappa_a - \kappa_b}{2\kappa_c}\right]^2 = \left(\frac{\kappa_a - \kappa_b}{2\kappa_c}\right)^2 + \frac{\kappa_d}{\kappa_c} \qquad (45a)$$

This in turn simplifies to the form

$$u_1^2 - u_1\left(\frac{\kappa_a - \kappa_b}{\kappa_c}\right) - \frac{\kappa_d}{\kappa_c} = 0 \qquad (45b)$$

Substitution of the rate ratio and equilibrium constants then gives

$$u_1^2 + u_1\left[\frac{k_{CA}K_{BC}}{k_{BC}}(K^{\dagger}_{CA}+1) - (K_{BC}+1)\right] - \frac{k_{CA}K_{BC}}{k_{BC}} = 0 \qquad (46)$$

Explicitly the rate ratio is

$$\frac{k_{CA}}{k_{BC}} = \frac{u_1[u_1 - (K_{BC}+1)]}{K_{BC}[1 - u_1(K^{\dagger}_{CA}+1)]} \geq 0 \qquad (47)$$

Since $u_1 > 0$, the limits stated above for the type III system are found by setting the rate ratio of Equation (47) equal to zero and to infinity.

EVALUATION OF EXPERIMENTAL DATA

Divariant Case

Any two of the three species may be designated, respectively, as components A and B, provided that neither $x_{AO} = x_{Ae}$ nor $x_{BO} = x_{Be}$. Experimental values of the concentrations x_A and x_B, at known values of the elapsed time, are required to calculate $1 - (F_B/F_A)$. A logarithmic plot of $|1 - (F_B/F_A)|$ vs. t is prepared on the same scale as Figures 7 and 8. This experimental plot is then superposed upon the appropriate one of these two figures, so as to obtain the best theoretical fit to the experimental data, and the following values are determined:

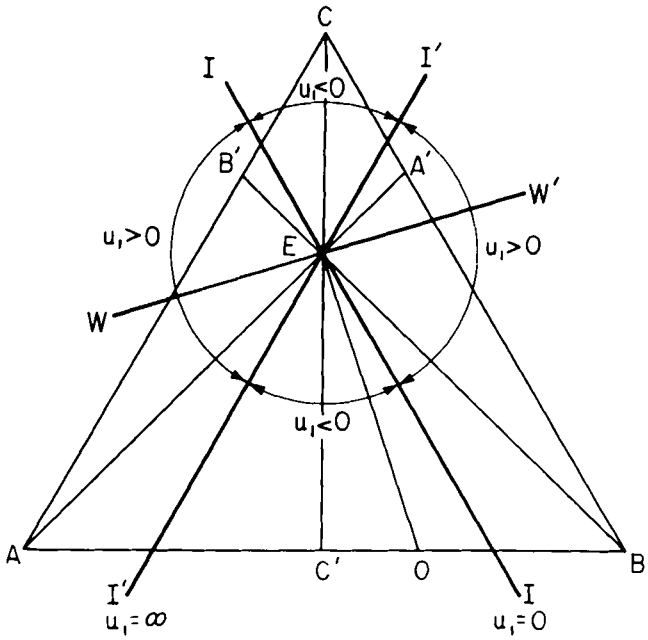

Fig. 9. Values of u_1 for various directions in which the reaction path might approach equilibrium.

1. The value of U for the contour.
2. The ratio $Q/[1-(F_B/F_A)]$, which can be obtained at the $Q = 1$ level, and from which u_1 can be determined by Equation (34) or (44). Now u_2 can be calculated from u_1 by Equation (10), and U can be verified from u_1 and u_2 together, by Equation (28). The degree of agreement between results 1 and 2 for U measures the accuracy of the fit and the satisfactoriness of the reaction model. [If the limiting ratio (F_B/F_A) is known, that is, if the straight-line reaction path has already been established, u_1 is known from Equation (44), and a single conversion-time point suffices to provide the rate coefficients.]
3. From the match on the abscissa scale, the value of $(\lambda_1 - \lambda_2)$ is obtained. If Figure 7 applies, T is available directly. If Figure 8 holds, U is used to determine $(T)_{Q=\infty}$ by Equation (41); then T/t is calculated as $(T)_{Q=\infty} \cdot T'/t$. The lumped rate parameter is then

$$\lambda_1 - \lambda_2 = (-U)T/t \qquad (48)$$

In terms of the intermediate parameters, $(\lambda_1 - \lambda_2) \equiv \sqrt{\Delta}$. The analysis up to this point thus provides a knowledge of $(\kappa_a - \kappa_b)$, κ_c, and κ_d, through Equations (6) and (7). This is not sufficient to determine λ_1 and λ_2 (or κ_a and κ_b) separately; the interdependence of the three terms is given by Equation (7). However, with u_1 known, recourse can be had to Equation (39*a*) or (39*b*). For example, a semilogarithmic plot of F_1 against t can be used to evaluate λ_1. Then λ_2 is determined immediately from the known value of $(\lambda_1 - \lambda_2)$. We note that the resulting lumped parameters u_1, u_2, λ_1, and λ_2 are sufficient to describe all reaction paths and reaction times for the given chemical system, without detailed calculation of the true rate coefficients. Nevertheless the individual coefficients can easily be determined if desired.

In principle, for a divariant system, as few as two experimental values of compositions along the reaction path will suffice for determining the rate ratios k_{BC}/k_{AB} and k_{CA}/k_{AB}. If the reaction times also are known for both the points, the method just outlined will give the rate ratios and the reference rate coefficient as well; in this case, indeed, the chord given by the two values of $(1 - F_B/F_A)$ plotted against t may fit many U contours, but the cross-check between u_1 (given by the ordinate) and U can be used iteratively to locate the appropriate value. Calculations based on Equations (39*a*) and (39*b*) can be used with these two points to determine both λ_1 and λ_2 independently of the Q vs. T plot. If the agreement on $\lambda_1 - \lambda_2$ is unsatisfactory, the apparent error can be allocated partly to the F's and partly to t's, to whatever extent seems appropriate, and the iteration for u_1 and U can be repeated.

It is of value to examine the limiting situation of using two given sets of compositions, without any time data, to establish the two rate ratios. Point 1, characterized by F_{A1} and F_{B1}, corresponds to a single infinitude of pairs of values of the rate ratios. Point 2 corresponds to another infinitude of such pairs. Thus point 1 gives rise to a curve of k_{CA}/k_{AB} vs. k_{BC}/k_{AB}, containing the allowable values; point 2 gives rise to a second such curve; and the parameters for their mutual reaction paths are given by the intersection of the two curves.

In rare cases, F_A and F_B (or related functions of concentration, such as x_A and x_B) may have been precalculated for the two pertinent K's and for a range of values of rate ratios. In such cases, construction of the rate ratio plot referred to above will be very simple.

The following iteration procedure is useful in improving the accuracy of a solution obtained by the master plot calculation. More generally, it can be used to generate a solution using composition data from runs having different starting compositions, and hence different H. Briefly, values of u_1 will be assumed, and the appropriate value of λ_2/λ_1 will be calculated for each given set of F_A and F_B values.

To proceed without reference to F_A and F_B, the assumed u_1 produces a value of u_2 by Equation (10). The values for each set of F_A and F_B are then introduced through the following relation, as obtained from Equations (39*a*) and (39*b*):

$$\frac{\lambda_2}{\lambda_1} = \frac{\ln F_2}{\ln F_1} = \frac{\ln [(F_A + u_2 H F_B)/(1 + u_2 H)]}{\ln [(F_A + u_1 H F_B)/(1 + u_1 H)]} \qquad (49)$$

For each assumed value of u_1, this procedure provides one point on each curve $(\lambda_2/\lambda_1$ vs. $u_1)$ drawn for an experimental pair of F_A and F_B values. After the intersection of the curves locates the acceptable u_1 and λ_2/λ_1, the two rate ratios can be calculated from them.

The master plot calculation is illustrated by the following example. A CSTR example presented later illustrates in a general way the above iteration procedure.

Example

Data from Haag and Pines (3) for the isomerization of *cis*-2-butene over sodium-alumina catalyst at 30°C.

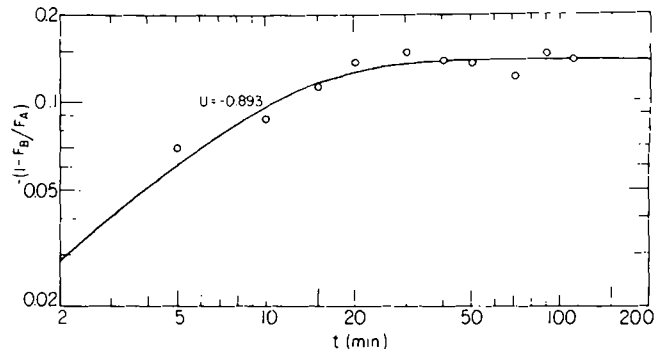

Fig. 10. Matching of experimental data for divariant example to a U contour on the master plot.

are given below, as smoothed values read from the published curves. Concentrations of x_C, representing 1-butene, are obtainable by material balance. The lumped rate coefficients and the individual rate coefficients are desired.

t, min.	x_A, *cis*-2-butene	x_B, *trans*-2-butene
0	1.0	0.0
5	0.905	0.045
10	0.853	0.088
15	0.800	0.129
20	0.755	0.170
30	0.678	0.245
40	0.610	0.324
50	0.549	0.392
70	0.438	0.517
90	0.347	0.612
110	0.288	0.678
∞	0.220	0.753

From the infinite time and initial values, the equilibrium constants and H are found to be

$$K_{AB} = 3.42 \qquad K_{BC} = 0.0361$$

$$K_{CA} = 8.08 \qquad H = -0.965$$

Values of $(1 - F_B/F_A)$ are calculated and plotted against time, as shown in Figure 10. The asymptotic value is

$$(1 - F_B/F_A)_{t=\infty} = -1/0.140$$

Then, by Equation (34)

$$u_1 H/(1 + u_1 H) = -1/0.140$$

$$u_1 = 0.909$$

From u_1, K_{BC}, and $K^{\dagger}_{CA}$, by Equation (10)

$$u_2 = -5.94$$

From u_1, u_2, and H, by Equation (28)

$$U = -0.893$$

The experimental data are matched to the $U = -0.893$ contour on the master plot (Figure 7), to give the ratio

$$T/t = 0.111$$

Then, by Equation (35)

$$\lambda_1 - \lambda_2 = 0.124$$

Values of F_1 and F_2 are calculated at various times and plotted on a logarithmic scale against time, as shown in Figure 11. A straight line is drawn through the points for F_1, and its slope gives

$$\lambda_1 = 0.139$$

Then, from $\lambda_1 - \lambda_2$

$$\lambda_2 = 0.015$$

A straight line with the slope of -0.015, shown in Figure 11, exhibits reasonable agreement with most values of F_2. Now u_1, u_2 λ_1, λ_2, and the equilibrium constants are used to determine the individual rate coefficients, expressed in units of min.$^{-1}$:

$$k_{AB} = 0.0093 \qquad k^{\dagger}_{AB} = 0.0027$$

$$k_{BC} = 0.0010 \qquad k^{\dagger}_{BC} = 0.0274$$

$$k_{CA} = 0.0950 \qquad k^{\dagger}_{CA} = 0.0118$$

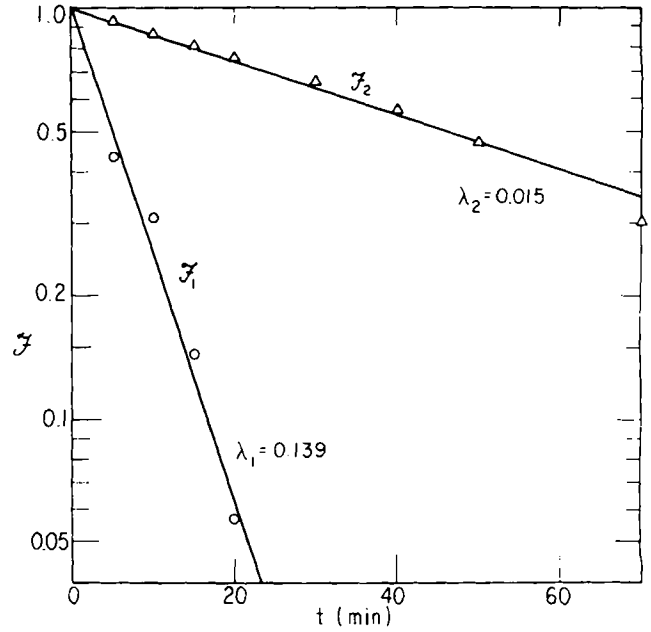

Fig. 11. Determination of λ_1 and λ_2 for divariant example.

Haag and Pines reported only values for the rate ratios; their values for the latter agree with those from the present fit to within ± 20%. This may well represent the limit of accuracy available from the original experimental data.

Monovariant Case

This case corresponds to one unknown rate ratio and one unknown reference rate coefficient. A reliable basis must exist for inferring that one potential reaction step, between two of the components, does not occur; so that the reaction system is truly monovariant. As stated above, a single composition for the reacting mixture, in addition to the starting point and the equilibrium, suffices to indicate the rate ratio; the reaction time for this single point then yields the rate coefficient.

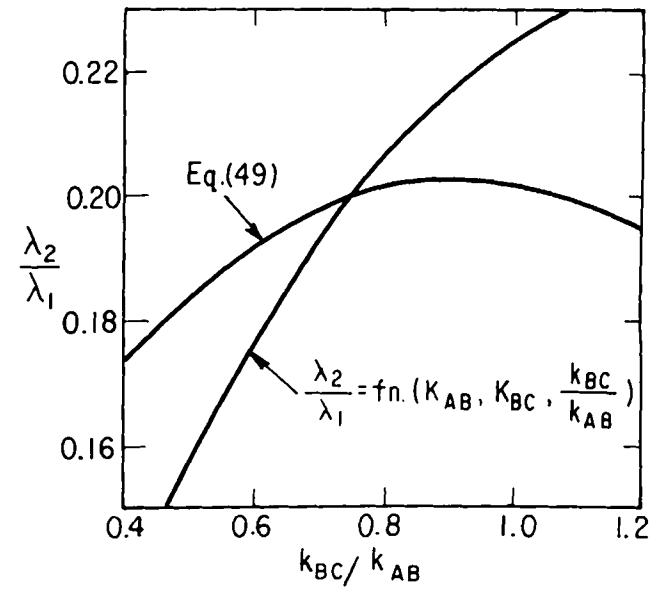

Fig. 12. Graphical solution for monovariant example.

If two or more points are available with their reaction times, it is advantageous to match them to the dimensionless plots of Figures 7 and 8. The product u_1u_2 now depends in a simple way upon the unknown rate ratio, which can be determined explicitly without further cross-plotting. Then $(\lambda_1 - \lambda_2)t$ can be used to determine the unknown rate coefficient.

If only a single mixture composition is available, its rate ratio can be evaluated by an iterative method similar to the one just described for a divariant system. A series of values of u_1 (and thus of the rate ratio itself) is assumed. By Equation (49), the known composition gives a value of the ratio λ_2/λ_1 for each input u_1. A match can then be sought either on λ_2/λ_1 (calculated both from composition and from the rate ratio based on the input u_1) or on the rate ratio (calculated both from u_1 directly, and from λ_2/λ_1 based upon u_1 and the composition).

Example

Isothermal kinetic data at constant density are given for the following monovariant system:

$$A \rightleftarrows B \rightleftarrows C$$

	x_A	x_B
Initial composition	1.000	0.000
Composition at $t = 0.10$	0.720	0.239
Equilibrium composition	0.200	0.200

(These are synthetic values, which, as will be seen, were computed from integer values of the parameters.) The lumped rate coefficients and the individual rate coefficients are desired. Equilibrium constants and H are calculated:

$$K_{AB} = 1.00 \qquad K_{BC} = 3.00 \qquad H = -4.00$$

At $t = 0.10$

$$F_A = 0.650 \qquad F_B = -0.195$$

Assumed values of k_{BC}/k_{AB} are used with the equilibrium constants to calculate λ_2/λ_1, u_1, and u_2. λ_2/λ_1 is also calculated by Equation (49). The two sets of values for λ_2/λ_1 vs. k_{BC}/k_{AB} are shown in Figure 12, which has the solution

$$\lambda_2/\lambda_1 = 0.200 \qquad k_{BC}/k_{AB} = 0.750$$

From Equation (39a)

$$\lambda_1 = 10.0 \qquad \lambda_2 = 2.0$$

λ_1 is a function of two equilibrium constants, the rate ratio, and k_{AB}. This is now solved to yield $k_{AB} = 4$; it follows that $k^{\dagger}_{AB} = 4$, $k_{BC} = 3$, and $k^{\dagger}_{BC} = 1$.

Accuracy of the Method

In the above method for evaluating experimental data, first, accuracy depends on the validity of first-order kinetics for the actual system. Second, errors in the direct method depend on the accuracy of graphing and reading the master plot, in which method visual weighting and averaging of points are adopted rather than a statistical procedure. Third, accuracy can be increased by iterating in the vicinity of the indicated results, to determine the most likely intersection point for the different curves, each corresponding to a different experimental point. As always, more data should give improved statistical accuracy. But use of the master plot, followed by iteration, makes maximum use of whatever number of data are available.

In the example from Haag and Pines, we believe our fit to be appreciably more accurate than theirs, due to the inherent smoothing and weighting of individual data in the present method. However, if the experimental system does not in fact correspond perfectly to first-order kinetics, neither their fit nor ours could be entirely correct.

DESIGN CALCULATIONS

Plots of Equation (30) or (31) are useful in predicting the course of a complex three-component system of first-order reactions, whether divariant or monovariant. The batch reaction time, or the tubular-reactor residence time under constant volume conditions, controls F_A and F_B through their dependence on $\lambda_1 t$. The proper curve is determined by λ_2/λ_1, which remains constant for a given chemical system at a single temperature, and by U or V, which depends not only upon constants u_1 and u_2 but also upon the given starting conditions as represented by H. Thus two parameters (U or V, and the ratio λ_2/λ_1) replace the three (two rate ratios and H) that would otherwise be needed to describe a divariant reaction.

Figure 13 shows F_A in terms of $\lambda_1 t$, for a specified value of λ_2/λ_1 ($= 0.6$) and several constant values of U ranging from $+10$ to -10. This figure can also be used to read F_B at constant V, for the indicated values of λ_2/λ_1 and $\lambda_1 t$. Similar figures are available for $\lambda_2/\lambda_1 = 0.01$, 0.03, 0.1, and 0.3, and are given in the Appendix.*

CONTINUOUS STIRRED-TANK REACTOR

Rate Equations

The rate in a CSTR is characterized by difference equations. For the general three-component system

$$\frac{x_A - x_{AO}}{t} = -(k_{AB} + k_{CA}K^{\dagger}_{CA})x_A + k_{AB}K^{\dagger}_{AB}x_B + k_{CA}x_C \tag{50a}$$

$$\frac{x_B - x_{BO}}{t} = k_{AB}x_A - (k_{AB}K^{\dagger}_{B} + k_{BC})x_B + k_{BC}K^{\dagger}_{BC}x_C \tag{50b}$$

$$\frac{x_C - x_{CO}}{t} = k_{CA}K^{\dagger}_{CA}x_A + k_{BC}x_B - (k_{CA} + k_{BC}K^{\dagger}_{BC})x_C \tag{50c}$$

Equations (50a) and (50b) are combined by elimination of residence time t and rearrangement as a linear equation in the three independent rate coefficients:

$$\alpha k_{AB} + \beta k_{BC} + \gamma k_{CA} = 0 \tag{51}$$

where

$$\alpha = (x_A - K^{\dagger}_{AB}x_B)(x_C - x_{CO}) \tag{52a}$$

$$\beta = (x_B - K^{\dagger}_{BC}x_C)(x_A - x_{AO}) \tag{52b}$$

$$\gamma = (x_C - K^{\dagger}_{CA}x_A)(x_B - x_{BO}) \tag{52c}$$

Equation (51) can be reduced to an equation of just the two rate ratios on division by k_{AB}:

$$\alpha + \beta\frac{k_{BC}}{k_{AB}} + \gamma\frac{k_{CA}}{k_{AB}} = 0 \tag{53}$$

To evaluate the rate ratios, at least two experimental CSTR runs are needed, in which the initial and final compositions are known in addition to the equilibrium composition. First the coefficients defined by Equations (52a), (52b), and (52c) are calculated for each experimental

* Figures for both tubular-flow and CSTR cases have been deposited as document 9607 with the American Documentation Institute, Photoduplication Service, Library of Congress, Washington, D. C., and may be obtained for $2.50 for photoprints or $1.75 for 35-mm. microfilm.

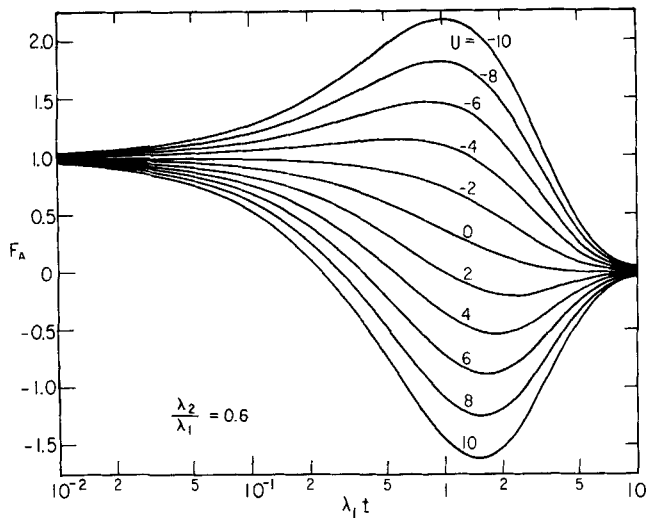

Fig. 13. Dimensionless concentration-time graph for predicting the yield of a reaction system with $\lambda_2/\lambda_1 = 0.6$.

run. Then the two equations that result from the substitution of these coefficients into Equation (53) are solved simultaneously to yield the two rate ratios. If data for more than two runs are available, a least-squares analysis can be used to determine the rate ratios. With one or more residence times known, Equations (50*a*), (50*b*), and (50*c*) can be used with the calculated rate ratios to determine the individual rate coefficients. Once the individual rate coefficients are known, the lumped rate coefficients λ_1, λ_2, u_1, and u_2 can be calculated for use in design equations.

In an alternate evaluation method, the lumped rate coefficients can be calculated in a manner analogous to the general iterative procedure for tubular-flow reaction. Wei (*10*) gives the solution for ratios F_1 and F_2 in a CSTR:

$$F_1 = \frac{F_A + u_1 H F_B}{1 + u_1 H} = \frac{1}{1 + \lambda_1 t} \qquad (54a)$$

$$F_2 = \frac{F_A + u_2 H F_B}{1 + u_2 H} = \frac{1}{1 + \lambda_2 t} \qquad (54b)$$

Solution for $\lambda_1 t$ and $\lambda_2 t$ in the above equations, followed by combination of the resulting equations with elimination of t, yields

$$\frac{\lambda_2}{\lambda_1} = \frac{F_2^{-1} - 1}{F_1^{-1} - 1} = \left[\frac{(1 - F_A) + u_2 H(1 - F_B)}{(1 - F_A) + u_1 H(1 - F_B)}\right]\left[\frac{F_A + u_1 H F_B}{F_A + u_2 H F_B}\right] \qquad (55)$$

The iteration method requires two or more experimental runs, preferably with different initial compositions. Experimentally determined initial, final, and equilibrium compositions are used to calculate H, F_A, and F_B for each run. Various values are assumed for u_1, from which u_2 is calculated by Equation (10) using the measured equilibrium conditions. For each experimental run, the set of u_1 and u_2 values is used with the respective H, F_A, and F_B to calculate a set of values for λ_2/λ_1 for that run, which is plotted against u_1. The point determined as the average intersection of the curves for all available runs gives the preferred values of u_1 and λ_2/λ_1.

Example

Kinetic and equilibrium data for a CSTR at a single temperature are given for a three-component reaction system:

	Initial composition			Final composition		
t	x_A	x_B	x_C	x_A	x_B	x_C
0.05	1.000	0.000	0.000	0.694	0.110	0.196
0.10	0.000	1.000	0.000	0.149	0.636	0.215
0.20	0.000	0.000	1.000	0.130	0.107	0.763
∞				0.200	0.200	0.600

(These are hypothetical values, predetermined for a given system in order to yield consistent results.) Values of the lumped rate coefficients are desired.

Values of H, F_A, and F_B are calculated for each run:

t	H	F_A	F_B
0.05	−0.25	0.618	0.450
0.10	−4.00	0.255	0.545
0.20	1.00	0.350	0.465

Equilibrium constants are calculated:

$$K_{BC} = 3.00 \qquad K_{CA}^{\dagger} = 3.00$$

Substitution into Equation (10) results in

$$u_2 = \frac{4 - u_1}{1 - 4u_1}$$

Various assumed values of u_1 are used to calculate values of u_2 by the above equation, and both used along with the set of H, F_A, and F_B values for each run to calculate F_1, F_2, and λ_2/λ_1 by Equations (54*a*), (54*b*), and (55) for that run. The resulting values of λ_2/λ_1 are plotted in terms of u_1 for each run in Figure 14. The intersection yields the solution

$$u_1 = -0.388 \qquad \lambda_2/\lambda_1 = 0.520$$

u_2 is calculated from u_1:

$$u_2 = 1.719$$

Equations (54*a*) and (54*b*) give values for λ_1 and λ_2:

$$\lambda_1 = 13.16 \qquad \lambda_2 = 6.84$$

The rate coefficients are then determined to be

$$k_{AB} = 4 \qquad k_{AB}^{\dagger} = 4$$

$$k_{BC} = 3 \qquad k_{BC}^{\dagger} = 1$$

$$k_{CA} = 2 \qquad k_{CA}^{\dagger} = 6$$

When the iteration method is used, it is important that the initial compositions for the experimental runs be varied in order to obtain a well-defined intersection, as in the above example. Equally important, such variation in the initial compositions yields rate coefficients that are characteristic of the complete reaction system rather than of just one area of the system. If the same initial composition is used for all experimental runs, much greater accuracy is required in the measurements in order to obtain equally accurate values for the rate coefficients.

As stated earlier, isothermal kinetic data taken on a tubular-flow reactor with different initial compositions can be used in the iterative procedure to provide a plot similar to Figure 18,* but with use of Equations (39*a*), (39*b*), and (49) instead of Equations (54*a*), (54*b*), and (55).

* See footnote on page 945.

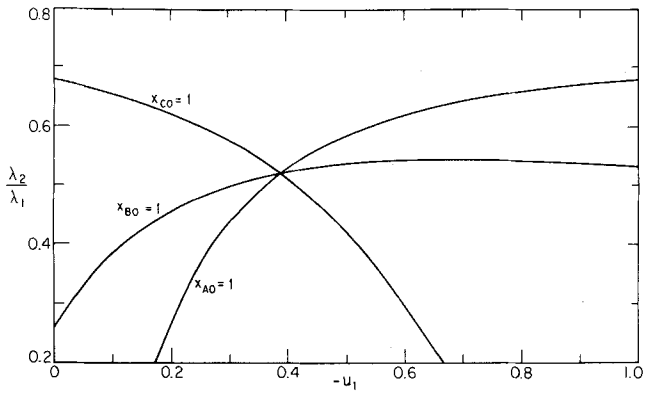

Fig. 14. Iterative solution for applicable values of λ_2/λ_1 and u_1 for CSTR example.

Variation in the initial compositions is just as important for the tubular-flow reactor as for the CSTR.

Design Calculations

As in the case of tubular-flow reactions, explicit formulas expressing F_A and F_B as functions of initial and equilibrium conditions, rate coefficients, and time can be derived for the CSTR. F_B is eliminated from Equations (54*a*) and (54*b*) by multiplying Equation (54*a*) by $(1 + u_1H)/u_1H$ and Equation (54*b*) by $(1 + u_2H)/u_2H$, followed by subtraction of one resulting equation from the other. F_A is then obtained explicitly:

$$F_A = \frac{u_2(1 + u_1H)}{(u_2 - u_1)(1 + \lambda_1 t)} - \frac{u_1(1 + u_2H)}{(u_2 - u_1)(1 + \lambda_2 t)} \tag{56}$$

Equation (28) can be used to replace u_1, u_2, and H:

$$F_A = \frac{1 + U}{1 + \lambda_1 t} - \frac{U}{1 + \lambda_2 t} \tag{57}$$

A similar equation is derived for F_B by eliminating F_A from Equations (54*a*) and (54*b*) upon subtraction, which results in

$$F_B = \frac{1 + u_1H}{(u_1 - u_2)H(1 + \lambda_1 t)} - \frac{1 + u_2H}{(u_1 - u_2)H(1 + \lambda_2 t)} \tag{58}$$

Substitution of V, defined by Equation (29), yields

$$F_B = \frac{1 + V}{1 + \lambda_1 t} - \frac{V}{1 + \lambda_2 t} \tag{59}$$

Equations (57) and (59) form the design equations for the CSTR. These equations differ from the design equations for the tubular-flow case, Equations (30) and (31), only in the form of the time dependence on the right side, reciprocal for the CSTR and exponential for the tubular-flow reactor. (This difference in form makes it impossible to develop a master plot for the CSTR that would be comparable to Figures 7 and 8. This same difference in the time dependence characterizes a single, irreversible, first-order reaction in the CSTR and tubular-flow cases.)

Plots of Equation (57) and (59) are useful in predicting the behavior of a three-component reaction system in a CSTR. Five figures in the Appendix show F_A in terms of $\lambda_1 t$ and of several contour values of U from $+10$ to -10, for specified values of λ_2/λ_1 (0.6, 0.3, 0.1, 0.03, 0.01). By substitution of V for U these figures also yield F_B as a function of V, λ_2/λ_1 and $\lambda_1 t$. Comparison of each CSTR curve with the corresponding tubular-flow curve shows that they coincide at small times. At large times they gradually spread apart, with the tubular-flow curve approaching equilibrium much faster.

ACKNOWLEDGMENT

Part of the results described were obtained in the course of an NSF Graduate Traineeship held by Larry E. Faith. The authors express their thanks to Edith P. Taylor and to William Kot for assistance in preparation of the manuscript. This study is part of a larger program on rate processes, supported by the National Science Foundation.

NOTATION

A, B, C, = chemical components
F_A, etc. = fractional approach of component A to its equilibrium concentration
F_1, etc. = function of F_A, F_B, u_1H; Equation (39). (F_1 corresponds to b_1/b_1^o as used by Wei and Prater.)
H = ratio of initial concentration differences from equilibrium, $(x_{BO} - x_{Be})/(x_{AO} - x_{Ae})$
K_{lm}, $K_{lm}^{\dagger}$ = equilibrium constant for (forward, reverse) reaction, $l \rightarrow m$
k_{lm}, $k_{lm}^{\dagger}$ = rate coefficient for (forward, reverse) reaction, $l \rightarrow m$; time^{-1}
Q = concentration function in dimensionless relation, Equation (34)
$\mathbf{R}$ = total rate vector
$\mathbf{R}_1$, $\mathbf{R}_2$ = constituent rate vector along characteristic path
$\mathbf{r}_{lm}$, etc. = rate vector for reaction $l \rightarrow m$
T, T' = time function in dimensionless relation, Equation (35) or (40)
t = time
U, V = parameters derived from u_1, u_2, and H; Equation (28) or (29); dimensionless
u_1, u_2 = lumped rate ratio parameter; dimensionless
x_A, etc. = mole fraction of A in the mixture $A + B + C$
Δ, κ_a, etc., λ_1, λ_2 = lumped rate coefficient parameters; time^{-1} or time^{-2}

Subscripts

O = starting condition
e = equilibrium
l = component reacted in given reaction
m = component formed in given reaction

LITERATURE CITED

1. Chermin, H. A. G., and D. W. van Krevelen, *Chem. Eng. Sci.*, **14**, 58 (1961).
2. Chien, J., *J. Am. Chem. Soc.*, **70**, 2256 (1948).
3. Haag, W. O., and Herman Pines, *ibid.*, **82**, 387 (1960).
4. Jost, Wilhelm, *Z. Naturforsch.*, **2a**, 159 (1947).
5. Jungers, J. C., "Cinétique Chimique Appliquée," Technip, Paris (1958).
6. Levenspiel, Octave, "Chemical Reaction Engineering," Wiley, New York (1962).
7. Lowry, T. M., and W. T. John, *J. Chem. Soc.*, **97**, 2634 (1910).
8. Rodiguin, N. M., and E. N. Rodiguina, "Consecutive Chemical Reactions," Van Nostrand, Princeton, N. J. (1964).
9. Siewert, H. R., P. N. Tenney, and Theodore Vermeulen, *U. S. Atomic Energy Comm. Rept. UCRL-10575*, Berkeley (1962).
10. Vriens, G. N., *Ind. Eng. Chem.*, **46**, 669 (1954).
11. Wei, James, *Can. J. Chem. Eng.*, **44**, 31 (1966).
12. ———, and C. D. Prater, *Advan. Catalysis*, **13**, 204 (1962).

Manuscript received September 1, 1966; revision received February 10, 1967; paper accepted February 13, 1967. Paper presented at A.I.Ch.E. Minneapolis meeting.